TECHNICAL REPORT

nature structural & molecular biology

In situ observation of protein phosphorylation by high-resolution NMR spectroscopy

Philipp Selenko[1,3], Dominique P Frueh[1], Simon J Elsaesser[1,3], Wilhelm Haas[2], Steven P Gygi[2] & Gerhard Wagner[1]

Although the biological significance of protein phosphorylation in cellular signaling is widely appreciated, methods to directly detect these post-translational modifications *in situ* are lacking. Here we introduce the application of high-resolution NMR spectroscopy for observing *de novo* protein phosphorylation *in vitro* and in *Xenopus laevis* egg extracts and whole live oocyte cells. We found that the stepwise modification of adjacent casein kinase 2 (CK2) substrate sites within the viral SV40 large T antigen regulatory region proceeded in a defined order and through intermediate substrate release. This kinase mechanism contrasts with a more intuitive mode of CK2 action in which the kinase would remain substrate bound to perform both modification reactions without intermediate substrate release. For cellular signaling pathways, the transient availability of partially modified CK2 substrates could exert important switch-like regulatory functions.

Post-translational protein modifications endow the proteome with the ability to establish, store and transduce information in response to cellular signaling events. Reversible protein phosphorylation, one of the most abundant protein modifications, dynamically regulates protein functions in many biological processes ranging from basic intracellular signaling events to cell proliferation, differentiation and programmed cell death. Unfortunately, the importance of post-translational protein phosphorylation stands in contrast to the difficulty of detecting these modifications *in vitro* and *in vivo*.

Common laboratory techniques to identify phosphorylated amino acids are limited in their ability to directly report the modification states of individual substrate sites and to resolve phosphorylated residues that are in close proximity to one another[1]. Radionucleotide incorporation experiments, in combination with mutant substrate analyses, for example, are time-consuming to perform and difficult to interpret when adjacent substrate sites are modified in a stepwise manner or when cross-talk between individual sites exists. Immunodetection with phospho-specific antibodies is equally limited by the requirement for comprehensive antibody libraries against all combinations of differentially modified epitopes. Phospho-specific antibodies are difficult to generate and often of poor discriminative quality. Similarly, the unambiguous identification of phosphorylated amino acids by mass spectrometry relies on the generation of uniquely modified peptide fragments by proteolytic digests. For regulatory protein sequences that harbor a large number of closely spaced modification sites, this is often not possible. In addition, all of the aforementioned methods require cell disruption, or cell fixation, as well as further sample preparation and purification steps in order to unambiguously identify modified substrate residues. Hence, these methods are not suitable for nondestructive investigations of cellular phosphorylation events in intact specimens.

The aim of our study was to determine the suitability of time-resolved, high-resolution NMR measurements for observing post-translational protein phosphorylation *in vitro* and *in vivo*. We reasoned that NMR spectroscopy would be ideally suited to detect *de novo* protein phosphorylation because protein resonance signals are highly sensitive to phosphorylation-induced changes in the environment of the respectively modified substrate residues. Indeed, NMR spectroscopy has recently been used to identify phosphorylated protein residues in a fragment of the human protein tau[2]. Another advantage of detecting protein phosphorylation by NMR spectroscopy is that the progressive establishment of these amendments can be monitored in a noninvasive and nondisruptive way. Protein phosphorylation reactions can therefore be analyzed in a continuous fashion and stepwise modification events dissected in a time-dependent manner. Furthermore, the modification of substrate residues by phosphorylation constitutes a covalent chemical addition that is not subject to exchange behaviors, unlike, for example, protein-protein interactions. Finally, phospho-modifications result in negligible mass increases, so that unmodified and modified substrate species are equally well detected. Together, these features predestine NMR spectroscopy as a new analytical tool for post-translational modification research.

In the present work, we report the dynamic establishment of multiple phospho-modifications within the regulatory region of the viral SV40 large T antigen. We specifically focus on phosphorylation reactions at adjacent substrate sites executed by the protein kinase casein kinase 2 (CK2), an abundant and constitutively active eukaryotic enzyme[3]. We first demonstrate the viability of our NMR approach with recombinant CK2 and model protein reporters *in vitro* and then

[1]Department of Biological Chemistry and Molecular Pharmacology and [2]Department of Cell Biology, Harvard Medical School, 240 Longwood Ave., Boston, Massachusetts 02115, USA. [3]Present addresses: Leibniz-Institut für Molekulare Pharmakologie, Robert-Rössle-Strasse 10, 13125 Berlin, Germany (P.S.) and Rockefeller University, 1230 York Avenue, New York, New York 10065, USA (S.J.E.). Correspondence should be addressed to P.S. (selenko@fmp-berlin.de) or G.W. (gerhard_wagner@hms.harvard.edu).

Received 23 September 2007; accepted 28 January 2008; published online 24 February 2008; doi:10.1038/nsmb.1395

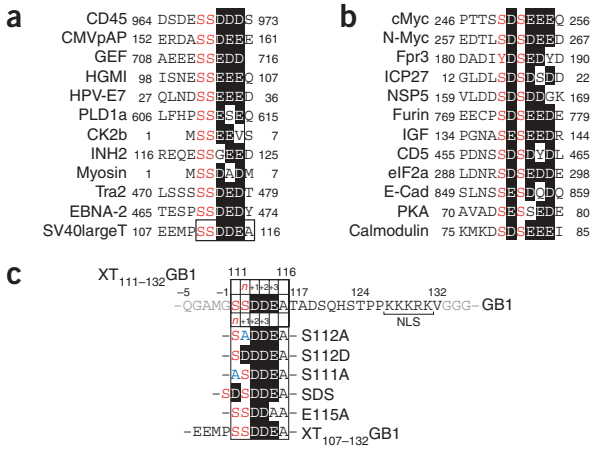

investigate the mechanistic properties of cellular CK2 and of endogenous modification events in cell-free extracts and inside live cells.

CK2 phosphorylates many cellular proteins, and their prominence in gene expression, signaling, RNA synthesis, apoptosis and cell transformation underscores the importance of this enzyme in universal cellular processes. CK2 modification sites frequently cluster in unstructured protein segments that often function as regulatory protein regions. Out of 175 annotated CK2 substrates[4], 23 have tandem phosphorylation sites at adjacent protein residues (12 of which are shown in **Fig. 1a**), whereas 25 have double modification sites separated by a single amino acid (12 of which are shown in **Fig. 1b**). For the majority of these CK2 substrates, the extent of phosphorylation at both modification sites is unknown.

Figure 1 Multiple sequence alignment of CK2 substrates containing tandem phosphorylation sites. (**a**) A selection of CK2 substrates with neighboring modification sites. Phosphorylatable amino acids are shown in red. The core acidic CK2 determinants, C-terminal to the dual CK2 sites, are shown in white on black. (**b**) CK2 substrates with two phosphorylation sites separated by a single amino acid. A more complete collection of CK2 substrates may be found in ref. 3. (**c**) Amino acid composition of the viral SV40 large T antigen regulatory region as it appears in the $XT_{111–132}$GB1 CK2 substrate. CK2 site residues Ser111 and Ser112 are shown in red. The Cdk1 substrate site Thr124 and the monopartite SV40 nuclear localization signal (NLS) are annotated (see text for details). Sequence compositions of SV40 mutants used in this study are shown below.

We chose the regulatory protein sequence of the viral SV40 large T antigen as a representative model CK2 substrate (**Fig. 1c**). CK2 phosphorylation of residues Ser111 and Ser112 of SV40 large T antigen has been shown to modulate the nuclear-import properties of the full-length protein, which are primarily mediated by the proximal monopartite nuclear localization sequence (NLS)[5,6]. Whereas Ser112 fulfills the stringent CK2 specificity requirements[7], which entail acidic residues at positions $n + 3$ and $n + 1$ (n being the phosphorylatable amino acid), Ser111 conforms to the $n + 3$ rule, but not to the $n + 1$ rule (**Fig. 1c**). Both residues harbor acidic neighbors at positions $n + 2$, which is the least stringent specificity determinant. In addition to these C-terminal kinase determinants, some CK2 substrates, including SV40 large T, contain negatively charged residues at positions $n - 1$ to $n - 4$. The functional roles of these N-terminal residues are much less well defined than for the C-terminal kinase determinants. They do not appear to be strictly required for CK2 activity, but have been shown to enhance the rate of phosphorylation in model CK2 peptide substrates[7]. Facing

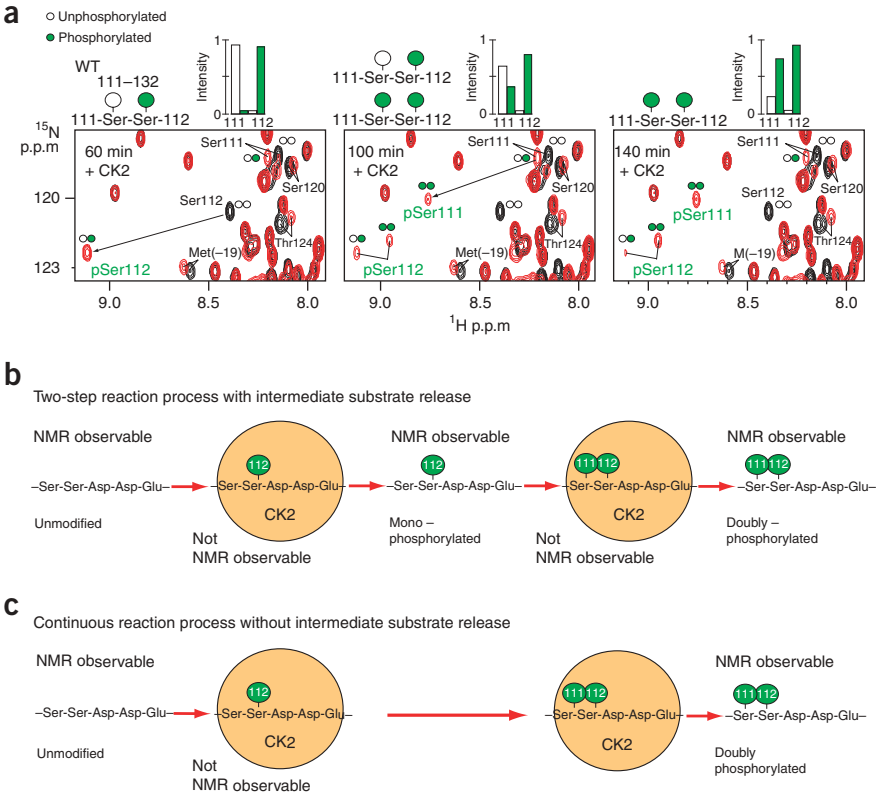

Figure 2 *In vitro* phosphorylation of $XT_{111–132}$GB1 by CK2. (**a**) Time-resolved 2D ^1H ^{15}N NMR experiments of ^{15}N-labeled $XT_{111–132}$GB1 in the presence of 500 enzymatic units of recombinant CK2. Progressive phosphorylation of $XT_{111–132}$GB1 by CK2 is shown by HSQC spectra obtained while the kinase reactions proceeded for the indicated times. In each panel, a selected region of the reference HSQC spectrum of unmodified $XT_{111–132}$GB1 (black) is overlaid with the spectrum of the mixture of $XT_{111–132}$GB1 with CK2, ATP and Mg^{2+} (red). Top panels indicate the degree of phosphorylation of Ser112 and Ser111 as quantified upon NMR signal integration. Double circles, phosphorylation states of Ser111 and Ser112 that give rise to the respective resonance peaks in the NMR spectra. Ser112 was completely phosphorylated after 60 min of CK2 incubation. Phosphorylation of Ser111 (100 min) resulted in changes in the chemical shifts of Ser111 and pSer112, indicating the progressive establishment of a mixed population of mono- and doubly phosphorylated species. After 140 min of CK2 incubation, most of $XT_{111–132}$GB1was doubly phosphorylated. (**b**) Schematic CK2 reaction mechanism involving a stepwise phosphorylation cascade and intermediate substrate release. (**c**) Alternative reaction profile for CK2 pursuing both phosphorylation steps in a continuous fashion and without intermediate release of the substrate.

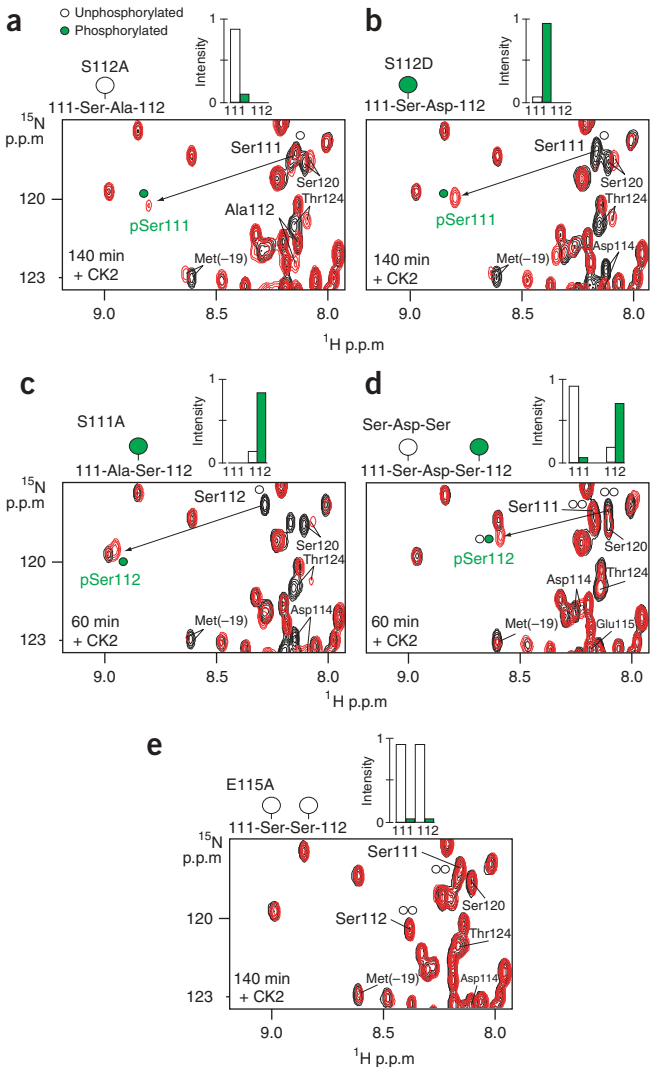

Figure 3 NMR analyses of mutant $XT_{111–132}GB1$ substrates. (**a**) Serine-to-alanine substitution of SV40 residue 112 (S112A) effectively suppressed phosphorylation of Ser111 by CK2 *in vitro*. (**b**) Mimicking phosphorylation at Ser112 by a serine-to-aspartate substitution (S112D) resulted in the rapid modification of Ser111. (**c**) A serine-to-alanine substitution of Ser111 (S111A) had no effect on the initial phosphorylation of Ser112. (**d**) Inserting an aspartic acid residue between Ser111 and Ser112 (Ser-Asp-Ser) still resulted in the preferential modification of Ser112. (**e**) Substituting Glu115 with alanine (E115A) completely abolished phosphorylation of Ser112 and Ser111 in the $XT_{111–132}GB1$ background.

this complexity, we wanted to determine which SV40 residues were essential for CK2 activity, whether CK2 indeed phosphorylated both residues of the SV40 substrate, whether it showed a preferred order of activity at these adjacent substrate sites and whether phosphorylation of one residue was mechanistically required for modification of the other.

RESULTS

CK2 phosphorylates Ser111 and Ser112 in a defined order

We incorporated the complete SV40 regulatory region (residues 111–132) into a model CK2 substrate ($XT_{111–132}GB1$). In this reporter, the B1 domain of streptococcal protein G (GB1) functioned as a C-terminal, solubility-enhancing protein tag[8]. We first confirmed the overall viability of $XT_{111–132}GB1$ as a target for recombinant CK2 using [γ-^{32}P]ATP radionucleotide incorporation experiments (data not shown). Next, we monitored the progressive phosphorylation of $XT_{111–132}GB1$ by consecutive, 2D heteronuclear single quantum coherence (HSQC) experiments with ^{15}N-labeled substrate in the presence of unlabeled CK2. For this reaction, $XT_{111–132}GB1$ (50 μM) was incubated with 500 enzymatic units of CK2 (1 μg) in a volume of 250 μl (final concentration of CK2, ~50 nM). For the first 60 min, CK2 exclusively phosphorylated Ser112 of $XT_{111–132}GB1$, which was manifested by a pronounced chemical shift change of the Ser112 resonance signal (**Fig. 2a**). The magnitude of the observed peak displacement was in agreement with the reported differences of chemical shift values between unphosphorylated and phosphorylated amino acids[9]. Phosphorylation of Ser112 proceeded until all substrate molecules were modified at this position (that is, no NMR signal of unphosphorylated Ser112 was detected). The modification of Ser111 began after the completion of Ser112 phosphorylation. At 100 min of CK2 incubation, we detected a mixed population of singly and doubly phosphorylated $XT_{111–132}GB1$ (**Fig. 2a**). Ser111 modification continued until all substrate molecules were phosphorylated at both sites (~140 min). Based on these experimental results we concluded that, *in vitro*, CK2 phosphorylated Ser112 and Ser111 in a distinct two-step reaction process. The kinase showed a clear order of processivity by exclusively modifying Ser112 first. Furthermore, because monophosphorylated $XT_{111–132}GB1$ was detected in the reaction mixture, CK2 must have dissociated from the partially modified substrate before it began to modify Ser111. The underlying rationale for this conclusion is as follows: because of the low abundance of CK2 in the reaction mixture (50 nM), and because of the large molecular weight of the resulting enzyme substrate complex (>140 kDa), any kinase-bound fraction of $XT_{111–132}GB1$ would not be detectable by NMR (**Fig. 2b**). Hence, all modified forms of $XT_{111–132}GB1$ represent 'free' substrate molecules that must have encountered the kinase but are no longer bound to it. If $XT_{111–132}GB1$ were to remain stably associated with the kinase for the duration of both modification steps, we would have observed only the finally released, doubly phosphorylated products (**Fig. 2c**). Therefore, because monophosphorylated, Ser112-modified $XT_{111–132}GB1$ was indeed present, the partially modified substrate must have dissociated from CK2 after the initial phosphorylation event. Furthermore, these observations also suggested that CK2 preferentially bound to unmodified $XT_{111–132}GB1$, even when Ser112-phosphorylated substrate molecules were present.

Phosphorylation of Ser111 depends on the modification of Ser112

Given the strict directionality of the observed CK2 reaction, we wanted to determine whether the modification of Ser111 required previous phosphorylation of Ser112. For this purpose, we substituted Ser112 with a unphosphorylatable amino acid (S112A). *In vitro*, the overall phosphorylation efficiency of this mutant was greatly reduced, although we did detect a residual NMR signal of modified Ser111 after prolonged CK2 incubation (**Fig. 3a**). This suggested that in the absence of a negative charge at the position $n + 1$, Ser111 of $XT_{111–132}GB1$ represented a poor CK2 substrate. Conversely, replacing Ser112 with aspartic acid (S112D) produced a CK2 substrate that was readily modified at Ser111 (**Fig. 3b**). As expected, a Ser111-to-alanine mutation (S111A) had no adverse effect on the initial modification reaction of Ser112 (**Fig. 3c**). Together, these data suggested that a negative charge at Ser112 was required to fulfill the $n + 1$ rule that enabled phosphorylation of the adjacent Ser111 by CK2. Following this hypothesis, we wondered whether the insertion of an aspartic acid

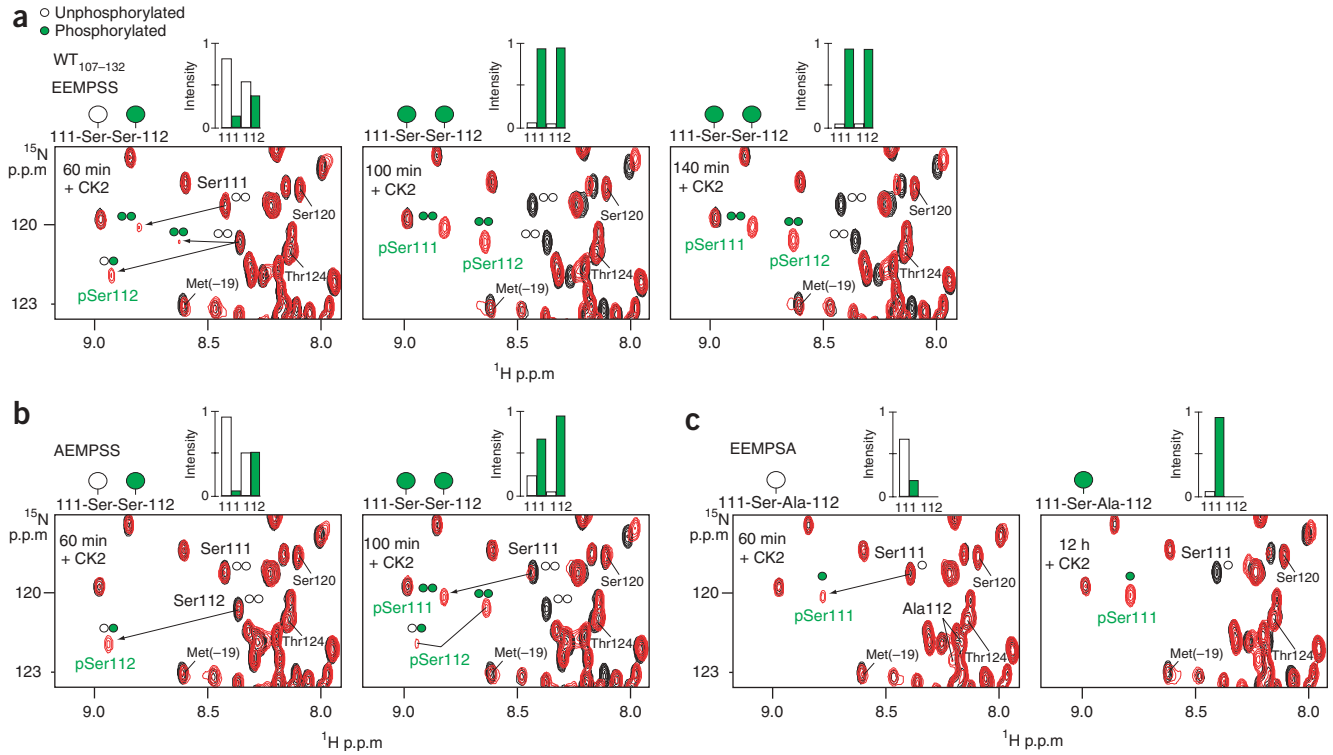

Figure 4 Time-resolved phosphorylation of $XT_{107–132}$GB1 by CK2. (**a**) Acidic residues N-terminal to the SV40 CK2 site (residues 107–110, EEMPSS) enhanced phosphorylation of Ser112 and Ser111. At 100 min of CK2 incubation, only doubly phosphorylated $XT_{107–132}$GB1 was detected. (**b**) Reducing the upstream net negative charge (E107A, yielding AEMPSS) resulted in an intermediate kinetic profile of Ser112 and Ser111 phosphorylation. (**c**) SV40 residues Glu107 and Glu108 (EEMPSA) partially restored phosphorylation of Ser111 in the S112A mutant background.

residue between Ser111 and Ser112 (Ser-Asp-Ser mutant) would create two equivalent CK2 target sites, as this construct would mimic tandem CK2 substrates with modification sites that are separated by a single amino acid (**Fig. 1b**). In the Ser-Asp-Ser mutant, both Ser111 and Ser112 contained acidic residues at positions $n + 3$ and $n + 1$ and hence simultaneously fulfilled all CK2 substrate specificity requirements[7]. Would insertion of a single negatively charged residue be sufficient to ablate the stringent directionality of CK2 and allow phosphorylation of both sites with equal efficiencies? Unexpectedly, this was not the case. As observed for the wild-type $XT_{111–132}$GB1 reporter, Ser112 was again completely modified before phosphorylation of Ser111 began (**Fig. 3d**). In analogy, we also mutated the most stringent CK2 specificity determinant, the acidic SV40 residue Glu115 at position $n + 3$ (E115A). Ser112 now conformed to the $n + 1$, but not to the $n + 3$ rule, whereas Ser111 fulfilled the $n + 3$ rule, but not the $n + 1$ rule. We analyzed the resulting CK2 reaction by NMR spectroscopy and found that neither Ser112 nor Ser111 became phosphorylated in this context and at any time of CK2 incubation (**Fig. 3e**). This indicated that Glu115 was absolutely required for phosphorylation of the $XT_{111–132}$GB1 substrate by CK2.

Role of N-terminal CK2 site residues

Although we had shown that acidic residues C-terminal to the adjacent SV40 substrate sites were sufficient to enable the stepwise phosphorylation by CK2, we wanted to investigate how negatively charged residues N-terminal to the phosphorylatable amino acids affected CK2's activity. To this end, we extended the $XT_{111–132}$GB1 substrate by residues $n - 1$ to $n - 4$ (Glu-Glu-Met-Pro) of the SV40 large T antigen and analyzed phosphorylation of the resulting $XT_{107–132}$GB1 protein by recombinant CK2 using NMR spectroscopy. Phosphorylated Ser112 was detected first (**Fig. 4a**). However, and in contrast to the sequence in the shorter construct (**Fig. 2a**), Ser111 modification began before the completion of Ser112 phosphorylation. Resonance peaks of unmodified, Ser112-phosphorylated, and doubly phosphorylated proteins were present within the first 60 min of the kinase reaction. At the equivalent incubation time, the shorter $XT_{111–132}$GB1 substrate was modified at Ser112 only (**Fig. 2a**). We verified that the observed enhancement in phosphorylation efficiency was due to the net charge at positions $n - 3$ and $n - 4$ by individually replacing the two glutamic acid residues with alanine. The E107A and the E108A mutant partially attenuated the observed effect and showed an intermediate kinetic profile (**Fig. 4b** and data not shown). Substituting both residues with alanine (E107A E108A) resulted in a stepwise modification behavior that was indistinguishable from that seen with the shorter $XT_{111–132}$GB1 protein (data not shown). We then asked whether the presence of Glu107 and Glu108 would restore Ser111 phosphorylation in the S112A mutant background. We introduced an analogous alanine substitution in the extended $XT_{107–132}$GB1 reporter and observed phosphorylation of S111, albeit at low levels (**Fig. 4c**). In contrast to the result seen with the shorter $XT_{111–132}$GB1 S112A substrate, prolonged incubation with CK2 (12 h) resulted in the full modification of Ser111 (**Fig. 4c**). Together, these data suggested that acidic residues N-terminal to the kinase phosphorylation sites contributed additively to the substrate's affinity for CK2. Although they did not alter the general mechanistic properties of the enzymatic reaction (that is, the order of activity and the intermediate release of partially modified substrates), they selectively enhanced the overall rate of phosphorylation.

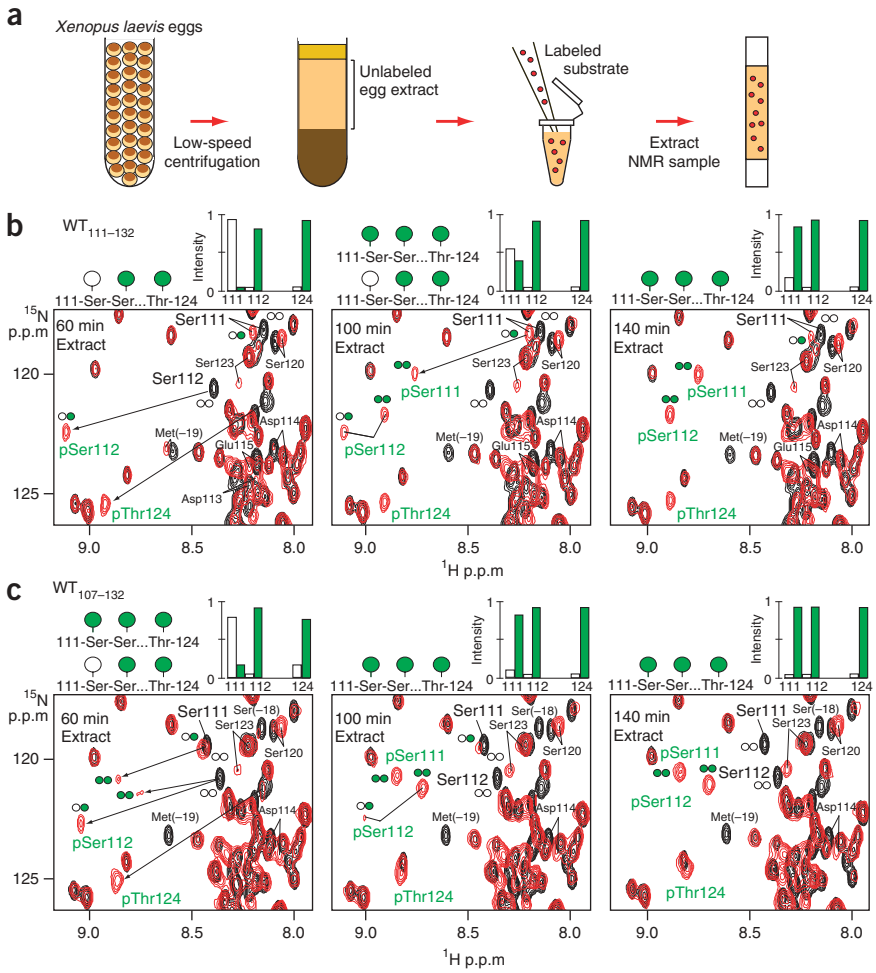

Figure 5 *De novo* phosphorylation of CK2 substrates in *Xenopus* egg extracts. (**a**) Overview of the preparation of extract NMR samples. (**b**) Time-resolved phosphorylation of $XT_{111–132}$GB1 by endogenous *Xenopus* kinases. The stepwise modification of Ser112 and Ser111 showed a reaction profile similar to that seen with 500 units of isolated CK2 *in vitro*. In addition, phosphorylation of Thr124 by endogenous kinases was readily apparent. (**c**) In comparison, the phosphorylation pattern of the N-terminally extended $XT_{107–132}$GB1 substrate indicated an increased rate of phosphorylation at equivalent time points. Phosphorylation of Thr124 was also detected for $XT_{107–132}$GB1.

Protein phosphorylation in *Xenopus* egg extracts

Having determined the mode of CK2 action for the $XT_{111–132}$GB1 substrate *in vitro*, we investigated whether the stepwise phosphorylation cascade of Ser112 and Ser111 was preserved under native *in vivo* conditions. We reasoned that the crowded cellular environment and the diminished diffusion of biomolecules inside intact cells[10] might enable CK2 to remain more stably associated with $XT_{111–132}$GB1 and to favor a continuous reaction mechanism without intermediate substrate release. Furthermore, we speculated that the excluded volume effect, a phenomenon typically encountered in crowded solutions[11], would increase the effective local concentrations of CK2 at Ser112-phosphorylated substrate molecules and concomitantly reduce the individual activation energies for the second phosphorylation step. In a first experiment, we resuspended $XT_{111–132}$GB1 in crude cellular extracts that we prepared from unfertilized *Xenopus laevis* eggs[12]. Endogenous CK2 is abundant in these extracts[13], and we confirmed Ser112 and Ser111 phosphorylation using [γ-^{32}P]ATP radionucleotide incorporation assays (**Supplementary Fig. 1a** online) and mass spectrometry (**Supplementary Fig. 1b**). Besides Ser112 and Ser111, endogenous kinases also phosphorylated Thr124 of the SV40 regulatory sequence. Thr124 constitutes a Cdk1 kinase site[14], which is another active enzyme in *Xenopus* egg extracts[15]. Further analyses confirmed that Thr124 constituted a bona fide Cdk1 substrate site and that phosphorylation of Ser112 and Ser111 by CK2 and that of Thr124 by Cdk1 occurred independently of each other (data not shown).

For time-resolved NMR analyses, we added ^{15}N-labeled $XT_{111–132}$GB1 to crude *Xenopus* egg extracts (**Fig. 5a**). Despite the large abundance of cellular proteins, the isotope-labeled protein substrate remained the only NMR-detectable species in this complex mixture. Of the two CK2 sites, Ser112 was phosphorylated first by endogenous *Xenopus* kinases, followed by Ser111 (**Fig. 5b**). The resulting chemical shift changes were indistinguishable from the observed peak displacement with recombinant CK2 (**Fig. 2a**). Moreover, the signal intensities of extract-phosphorylated $XT_{111–132}$GB1 were comparable to those in the respective *in vitro* NMR experiments, which demonstrated that the endogenous enzymatic reaction likely proceeded via a similar two-step mechanism with intermediate release of the substrate. Phosphorylation of Thr124 resulted in a large chemical shift change of this residue, which was reminiscent of the phosphorylation-induced peak displacements of Ser112 and Ser111 (**Fig. 5b**). Furthermore, all $XT_{111–132}$GB1 mutants showed extract modification patterns that were similar to the ones observed *in vitro* (**Supplementary Fig. 2a** online). These extract NMR results were further confirmed by [γ-^{32}P]ATP radionucleotide incorporation assays (**Supplementary Fig. 2b**), and they suggested that the *in vitro*–determined phosphorylation characteristics for the different $XT_{111–132}$GB1 reporters were collectively preserved in crude *Xenopus* egg extracts.

How did the N-terminally extended $XT_{107–132}$GB1 substrate behave in *Xenopus* egg extracts? NMR analyses revealed that the overall reaction profile for the stepwise modifications of Ser112 and Ser111 was preserved under these conditions (**Fig. 5c**). Compared to the shorter $XT_{111–132}$GB1 protein (**Fig. 5b**), $XT_{107–132}$GB1 showed an increased rate of phosphorylation at equivalent time points. However, this effect was less pronounced than with recombinant CK2 *in vitro* (**Fig. 4a**). We then asked whether the simultaneous addition of both CK2 reporters to *Xenopus* egg extracts would result in the preferential modification of one substrate over the other. If the different phosphorylation efficiencies of $XT_{111–132}$GB1 and $XT_{107–132}$GB1 were indeed caused by differences in CK2 affinity, then the two substrates would directly compete for endogenous CK2, sequester the cellular enzyme to different extents and consequently show individual phosphorylation profiles that differed from those of their 'isolated' forms. Such an experimental outcome would provide an example of a classical 'systems-level effect': that is, the presence of the high-affinity

substrate would suppress phosphorylation of the low affinity substrate through direct competition for access to the kinase[16]. NMR analyses of an equimolar mixture of ^{15}N-labeled $XT_{111–132}$GB1 and $XT_{107–132}$GB1 in *Xenopus* egg extracts revealed that after 140 min of extract incubation, Ser112 and Ser111 of the extended $XT_{107–132}$GB1 substrate were fully phosphorylated (**Supplementary Fig. 3** online). In contrast, the initial phosphorylation reaction of Ser112 of $XT_{111–132}$GB1 was in progress and NMR signals of unmodified Ser112 as well as of phosphorylated Ser112 were present. Note that in the absence of $XT_{107–132}$GB1, both Ser112 and Ser111 of $XT_{111–132}$GB1 were completely phosphorylated at this time (**Fig. 5b**). Even after prolonged extract incubation (>3 h), no double phosphorylation of Ser112 and Ser111 was detected for $XT_{111–132}$GB1 (data not shown). These observations demonstrated that the presence of acidic residues N-terminal to the SV40 CK2 substrate sites could selectively enhance the phosphorylation efficiency of otherwise identical protein sequences. They also indicated that the individual lifetimes of partially modified CK2 substrates were variable and depended on the presence of other CK2 targets. Together, this suggested that the effective degree of CK2 phosphorylation of different substrate molecules was determined by their individual kinase affinities and by their relative concentrations with respect to other CK2 targets.

In vivo protein phosphorylation in *Xenopus* oocytes

Finally, we studied the phosphorylation behavior of native CK2 in intact *Xenopus laevis* oocytes. Although *Xenopus* oocytes represent a different biological environment than *Xenopus* eggs[15], CK2 is equally abundant and active in both cell types[13]. In contrast, Cdk1 is known to be inactive in mature oocytes[17]. We microinjected ^{15}N-labeled $XT_{111–132}$GB1 into freshly prepared cells and conducted time-resolved in-cell NMR experiments as reported[18] (**Fig. 6a**). In this *in vivo* setting, we also observed the stepwise phosphorylation cascade of Ser112 and Ser111 and the intermediate release of Ser112-phosphorylated substrate (**Fig. 6b**). In accordance with Cdk1 being inactive in stage VI oocytes, we detected no Thr124 phosphorylation. Together, these findings suggested that despite the highly crowded, intracellular environment of live oocyte cells, endogenous CK2 preferentially phosphorylated the unmodified $XT_{111–132}$GB1 substrate, rather than the partially modified product. The same was true for the N-terminally extended $XT_{107–132}$GB1 substrate (data not shown). We then asked whether $XT_{111–132}$GB1-injected oocytes would be capable of maturing into fertilizable *Xenopus* eggs. Oocyte to egg maturation can be triggered by the external addition of progesterone, which results in Cdk1 activation, germinal vesicle breakdown and the resumption of the first and second meiotic cycle[15]. Upon addition of progesterone to $XT_{111–132}$GB1 injected oocytes, time-resolved in-cell NMR experiments revealed the progressive phosphorylation of Thr124 (**Fig. 6c**). This event coincided with the formation of a white spot on the darkly pigmented animal poles of *Xenopus* oocytes, which serves as a well established indicator for oocyte to egg maturation[15]. No Thr124 phosphorylation was observed in control cells not stimulated by progesterone (data not shown). At all times, the phosphorylation states of Ser111 and Ser112 remained unchanged, thus indicating that these CK2-dependent phosphorylation patterns were preserved during maturation from oocyte to egg and that $XT_{111–132}$GB1-injected oocytes were viable and cell-cycle competent. Overall we concluded that the mechanistic *in vitro* properties of Ser112 and Ser111 phosphorylation were preserved *in vivo*.

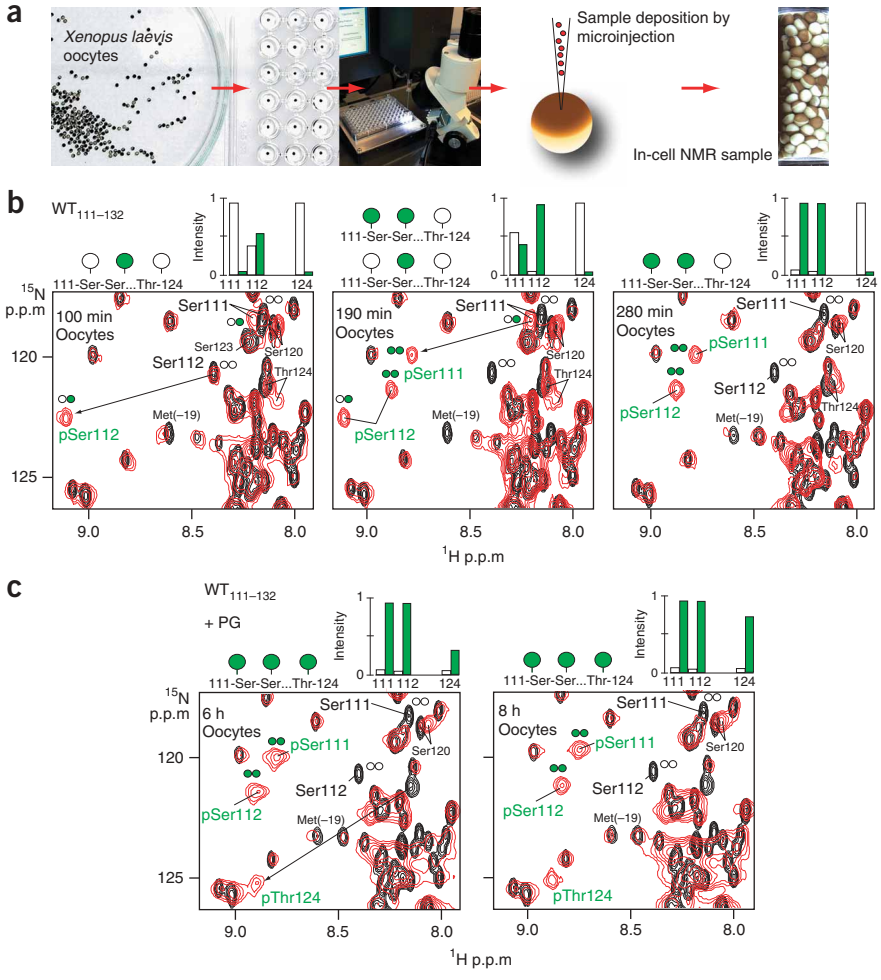

Figure 6 *In vivo* phosphorylation of $XT_{111–132}$GB1 in *Xenopus laevis* oocytes. (**a**) Overview of the in-cell NMR sample preparation scheme using intact *Xenopus* oocyte cells. (**b**) Time-resolved phosphorylation of $XT_{111–132}$GB1 in live cells. In-cell NMR experiments of $XT_{111–132}$GB1-injected oocytes show the *in vivo* phosphorylation of Ser112, followed by the phosphorylation of Ser111. (**c**) Progressive Thr124 phosphorylation after progesterone (PG) addition to $XT_{111–132}$GB1-injected oocytes.

DISCUSSION

Protein phosphorylation at multiple, closely spaced substrate sites is a frequent event in cellular signaling whereby stimuli of different origins and intensities can communicate with each other to give rise to potentiated or attenuated biological responses. Often, the protein kinases involved are acidophilic and/or phosphate-directed in nature, so the generation of phosphorylated amino acids

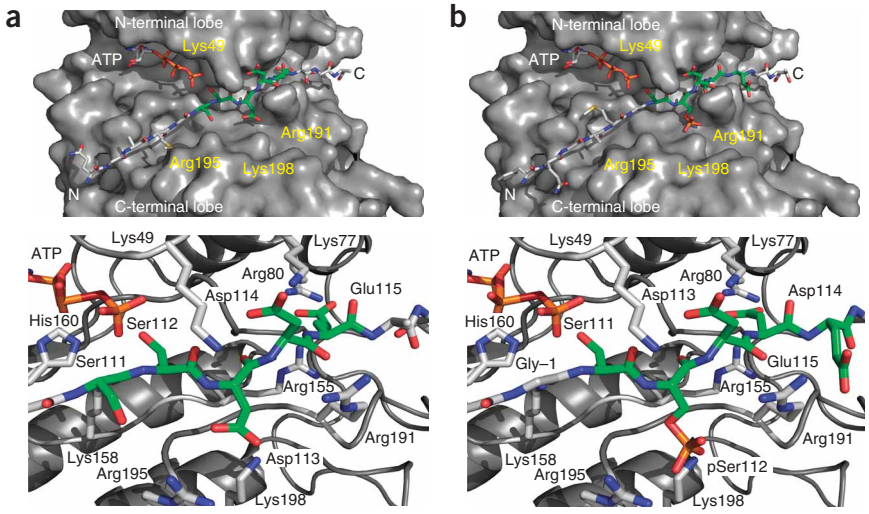

Figure 7 Modeled interactions of $XT_{111–132}GB1$ with the catalytic subunit of CK2. (**a**) The hypothetical peptide conformation of the first CK2 phosphorylation reaction at Ser112. Top panel, surface rendering of the CK2α catalytic cleft (gray) with bound substrate and ATP. For clarity, only residues Gln(–5) to Gly(–1) of the N-terminal linker in $XT_{111–132}GB1$ and SV40 residues Ser111–Thr117 are displayed as sticks. Green, amino acids comprising the CK2 substrate site (Ser111, Ser112) and the downstream specificity determinants (Asp113–Glu115). The CK2 substrate spans the C- (bottom) and N-terminal (top) lobes of CK2α in an extended conformation. Bottom panel, close-up of the catalytic core of the kinase. Gray, ribbon representation of CK2α; sticks, amino acid side chains forming the basic network of residues coordinating the substrate. Ser112 is positioned toward the distal phosphate moiety of ATP in order to function as the primary phospho-acceptor. Charge complementation of acidic CK2 determinants by basic residues of CK2α is readily visible. (**b**) Model of the second modification step, with Ser112-phosphorylated $XT_{111–132}GB1$ bound to CK2α. Overall, the substrate peptide is register-shifted by one amino acid in order for Ser111 to function as the phospho-acceptor. Bottom, close-up as in **a**.

creates or potentiates the consensus for the kinase itself. Although the physiological relevance of such processive phosphorylation events is generally appreciated and has been intensively investigated at the cellular level, the mechanistic aspects of these reactions are poorly understood. Our data revealed that the ubiquitous protein kinase CK2 phosphorylated residues Ser112 and Ser111 of the regulatory region of the viral SV40 large T antigen in a preferred order and with intermediate release of the substrate, both *in vitro* and *in vivo* (**Fig. 2b**). Given the close proximity of these phosphorylatable amino acids, this dual-encounter, distributive mechanism is in contrast to a more intuitive, processive reaction behavior in which CK2 would thread along the substrate to perform both modification steps without intermediate substrate release ('bind-and-slide' mechanism) (**Fig. 2c**). Another example of a distributive, two-step kinase reaction profile at neighboring substrate sites is the activating phosphorylation reaction of p42/MAPK (mitogen-activated protein kinase) by the upstream protein kinase MAPKK[19]. In this case, MAPKK phosphorylates Tyr190 and Thr188 of MAPK in a sequential order and through a similar dual-encounter mechanism that involves the release of the initially Tyr190-modified, monophosphorylated substrate. Although the paper in question pointed out the importance of distributive kinase mechanisms in ultrasensitive switch-like responses, and the overall gain in signaling fidelity by avoiding false activation events through aberrant phosphorylation steps[19], it did not discuss the notion that partially modified substrates may themselves function as binding partners for different proteins, or as activators of different signaling pathways. As we have shown for CK2, the individual lifetimes of intermediately modified substrate species can vary greatly, depending on the relative amounts and affinities of other substrate molecules that are present. During periods of elevated cellular protein synthesis, for example, new CK2 substrates might be available in high abundance and in various modification states. At those times, partially modified CK2 targets could selectively bind to different scavenging proteins, whose functions would then be modulated in CK2 substrate–specific ways. For a constitutively active protein kinase like CK2, this mode of action may be important in regulating the biological outcome of cellular signaling pathways.

Can we explain CK2's phosphorylation behavior at adjacent substrate sites by the available structural information on CK2 enzyme–substrate complexes? We mapped the unphosphorylated SV40 peptide onto a recently proposed model of a complex between CK2α and a phospho-acceptor peptide[20]. In what we reasoned could represent the substrate conformation that leads to Ser112 phosphorylation, $XT_{111–132}GB1$ docked into the catalytic cleft between the N- and C-terminal lobes of CK2α, with interactions across both halves of the catalytic subunit (**Fig. 7a**). The hydroxyl group of the phospho-acceptor Ser112 was positioned toward the distal phosphate moiety of bound ATP, whereas the preceding Ser111 pointed away from the active site. In this conformation, acidic residues Asp113 (n + 1), Asp114 (n + 2) and Glu115 (n + 3) of SV40 were charge-complemented by basic amino acids of CK2 that are known to be required for substrate recognition[21]. These include residues Lys74–Arg80, Arg155 and Lys158 of CK2α. Further positive charges within the kinase N terminus (Lys49) and the activation segment (Arg191, Arg195 and Lys198) additionally stabilized these interactions. In a model of the kinase-substrate complex responsible for the second modification step, modified Ser112 was register-shifted by one amino acid in order for Ser111 to function as the phosphorylatable amino acid (**Fig. 7b**). Phosphorylated Ser112 replaced Asp113, which in turn was located in the position that was occupied by Asp114 in the first reaction step. The basic network of CK2α residues 74–80 now coordinated Asp114 instead of Glu115. Both models revealed that residues Lys49 and Arg191 of CK2α accommodated the SV40 peptide in a tight, clamp-like interaction. In mutational analyses, these two residues have been shown to be essential for substrate recognition[21]. Given the overall extended conformation of $XT_{111–132}GB1$, with side chain moieties pointing in opposite directions, a continuous threading mechanism to perform both phosphorylation steps without substrate release would necessitate large changes in the $XT_{111–132}GB1$ backbone geometry with concomitant side chain flips. As was evident from the modeled structures, such conformational alterations could not be easily accommodated without substantial rearrangements of both CK2α lobes. However, such conformational reorganizations might also lead to substrate release. How exactly CK2 dissociates from partially or fully phosphorylated substrate molecules remains an open question. Here,

the conformational properties of the ATP recharging reaction and CK2α's interactions with the regulatory CK2β subunit of the tetrameric holoenzyme are likely to be important[22].

How general a phenomenon is the stepwise phosphorylation behavior of CK2 at adjacent substrate sites? As our study only used a single substrate type and a minimal consensus sequence for CK2 activity, the data will only partially reflect the behavior of full-length CK2 substrates. Indeed, most kinase targets harbor further regulatory domains[23] or remote kinase docking sites[24] that ultimately dictate the individual modification behaviors, and it is well known that interactions between phospho-acceptors and protein kinases rely only in part on the minimally required consensus sequences. In that sense, the phosphorylation characteristics of CK2 determined here may represent the core mechanistic properties of this enzyme, with variations brought about by contributions in *cis*, for full-length protein substrates, or in *trans*, through other scaffold, anchor or adaptor proteins[25]. Different CK2 phosphorylation characteristics at tandem modification sites, depending on whether full-length protein substrates or substrate fragments were used, have indeed been reported for Fpr3 (ref. 26) and calmodulin[27], two examples also listed in **Figure 2b**. Note particularly, however, that the NMR approach described here is not *per se* restricted to phosphorylation studies of fragmented protein substrates only. We deliberately chose these model reporters to most accurately define the basic mechanistic phosphorylation properties of CK2 at adjacent substrate sites. Other *in vitro* and *in vivo* NMR phosphorylation studies on full-length protein substrates have indeed indicated the general feasibility of such analyses (unpublished data).

In summary, the application of high-resolution NMR spectroscopy to analysis of protein phosphorylation *in vitro* and *in vivo* provides many advantages over traditional methods. First, it enables the direct detection of phosphorylated substrate residues irrespective of their actual number or position in the substrate protein. Second, it allows phosphorylation reactions to be studied over arbitrary periods of time and without having to disrupt the systems under investigation. Third, it provides quantitative information about individual phosphorylation states because the magnitudes of the respective NMR signals unambiguously report the amounts of modified versus unmodified substrate molecules. Fourth, it enables noninvasive analyses of the establishment of these covalent amendments in cell-free extracts and inside live cells. It can be used to directly study protein phosphorylation under native conditions *in vivo* and during defined cellular events, such as the progression through different stages of the cell cycle, or upon the stimulation of intracellular signaling pathways by external factors. Finally, the NMR approach presented here should in principle be applicable to observe other types of post-translational protein modifications, such as protein methylation or acetylation. We are currently exploring these possibilities.

METHODS

Preparation and NMR assignment of CK2 substrates. We inserted wild-type SV40 large T antigen residues 111–132 into a modified pET9d vector that harbored the streptococcal protein G B1 domain (56 residues)[18]. The resulting CK2 substrate ($XT_{111–132}$GB1, ~10 kDa) contained MKHHHHHHPMSDY DIPTTENLYFQGAMG N-terminal to the respective SV40 residues, and a three-glycine linker connected this extended peptide to the globular GB1 domain. All mutant constructs were generated by site directed mutagenesis and verified by DNA sequencing. We prepared isotope-labeled and unlabeled substrates in *Escherichia coli* by standard protocols and in the appropriate minimal growth media[18]. We used triple-resonance backbone methods[28–30], in combination with nonuniform sampling schemes[31], for complete NMR assignment. For the unambiguous NMR assignment of new resonance signals of phosphorylated $XT_{111–132}$GB1, we incubated ^{13}C-, ^{15}N-labeled protein in *Xenopus* egg extracts until both unmodified and partially modified species were present (as determined by 2D HSQC experiments). We then purified the mixed population of $XT_{111–132}$GB1 from these extracts and repeated backbone NMR experiments.

[γ-^{32}P]ATP incorporation experiments. We assayed phosphorylation of $XT_{111–132}$GB1 and mutant constructs by standard protocols with recombinant CK2 or in *Xenopus* egg extracts. Modified substrates were purified at the indicated time points using Ni-NTA beads, washed and separated by SDS-PAGE. We quantified [γ-^{32}P]ATP incorporation by phosphorimager scanning and determined overall protein abundances by western blotting using antibodies to GB1.

Time-resolved *in vitro*, extract and in-cell NMR experiments. *In vitro* kinase reactions were reconstituted with 50 μM of ^{15}N-labeled substrates and recombinant human CK2, 500 enzymatic units, in the presence of ATP (0.5 mM) and Mg_2SO_4 (0.1 mM). We acquired consecutive ^1H, ^{15}N HSQC correlation spectra while the kinase reaction proceeded. All NMR experiments were recorded at 295 K on a Bruker Avance 600 MHz NMR spectrometer equipped with a cryoprobe. NMR data were recorded with 16 transients and 1,024 (^1H) × 64 (^{15}N) complex points (43 min of acquisition time). For time-resolved NMR experiments, we acquired a series of four consecutive HSQC experiments without interruption (60 min, 100 min, 140 min and 180 min). Sample preparation required ~15 min before NMR data acquisition. NMR samples in *Xenopus* egg extracts and intact oocytes were prepared essentially as described[18]. Injection of ^{15}N-labeled substrates was adjusted to yield 'cellular' concentrations of 50 μM (assuming an oocyte cell volume of 1 μl). We recorded time-resolved NMR spectra in extracts with spectrometer settings identical to those of the respective *in vitro* NMR experiments with recombinant CK2. In-cell NMR spectra in *Xenopus* oocytes were acquired with 32 transients and 1024 (^1H) × 64 (^{15}N) complex points (~90 min of acquisition time).

Mass spectrometry. For mass determination of intact $XT_{111–132}$GB1, we analyzed the protein using nanoscale LC-ESI-FTIR-MS. To identify modified amino acid residues, we incubated $XT_{111–132}$GB1 in *Xenopus* egg extracts for ~90 min to yield a mixture of unmodified and modified substrate. The proteins were isolated by histidine-tag purification and separated by SDS-PAGE. We digested Coomassie-stained gel bands with trypsin and analyzed the resulting peptide mixtures by LC-MS/MS using the LTQ FT setup described previously[32]. MS/MS spectra were assigned by searching them against the amino acid sequence of $XT_{111–132}$GB1 using the SEQUEST algorithm[33]. The probability for the correct localization of phosphorylation sites was calculated as described[34].

Model building. We built the CK2α $XT_{111–132}$GB1 substrate complexes using PyMOL (http://pymol.sourceforge.net) starting from the CK2α substrate model reported[20]. For subsequent rounds of structure refinements in XPLOR[35], we kept the CK2α moiety rigid and replaced the AMP-PNP cofactor of the original model with ATP.

Note: Supplementary information is available on the Nature Structural & Molecular Biology website.

ACKNOWLEDGMENTS

We are most grateful to J. Ruderman and to members of her group, especially E. Chung and M. Lai, for continuous support in all aspects of our *Xenopus* work. We thank K. Niefind and O.G. Issinger for providing the PDB coordinates of the peptide substrate CK2α model that we used as the starting structure for building the SV40-CK2α models. We also thank J. Sun for help with XPLOR to calculate the final models. P.S. gratefully acknowledges funding by the Human Science Frontier Program Organization (long-term fellowship LT00686/2004-C) and by the Max Kade Foundation. This work was also funded by grant GM47467 of the US National Institutes of Health to G.W.

AUTHOR CONTRIBUTIONS

P.S. conceived the project, devised and performed the biochemical and NMR experiments and wrote the manuscript. D.P.F. performed NMR experiments and

wrote the manuscript. S.J.E. performed biochemical experiments and read and approved the manuscript and the conclusions drawn therein. W.H. performed MS experiments and approved the manuscript and the conclusions drawn therein. S.P.G. and G.W. read and approved the manuscript and the conclusions drawn therein.

Published online at http://www.nature.com/nsmb/
Reprints and permissions information is available online at http://npg.nature.com/reprintsandpermissions

1. Salih, E. Phosphoproteomics by mass spectrometry and classical protein chemistry approaches. *Mass Spectrom. Rev.* **24**, 828–846 (2005).
2. Landrieu, I. *et al.* NMR analysis of a Tau phosphorylation pattern. *J. Am. Chem. Soc.* **128**, 3575–3583 (2006).
3. Pinna, L.A. Protein kinase CK2: a challenge to canons. *J. Cell Sci.* **115**, 3873–3878 (2002).
4. Meggio, F. & Pinna, L.A. One-thousand-and-one substrates of protein kinase CK2? *FASEB J.* **17**, 349–368 (2003).
5. Hubner, S., Xiao, C.Y. & Jans, D.A. The protein kinase CK2 site (Ser111/112) enhances recognition of the simian virus 40 large T-antigen nuclear localization sequence by importin. *J. Biol. Chem.* **272**, 17191–17195 (1997).
6. Rihs, H.P., Jans, D.A., Fan, H. & Peters, R. The rate of nuclear cytoplasmic protein transport is determined by the casein kinase II site flanking the nuclear localization sequence of the SV40 T-antigen. *EMBO J.* **10**, 633–639 (1991).
7. Kuenzel, E.A., Mulligan, J.A., Sommercorn, J. & Krebs, E.G. Substrate specificity determinants for casein kinase II as deduced from studies with synthetic peptides. *J. Biol. Chem.* **262**, 9136–9140 (1987).
8. Zhou, P., Lugovskoy, A.A. & Wagner, G. A solubility-enhancement tag (SET) for NMR studies of poorly behaving proteins. *J. Biomol. NMR* **20**, 11–14 (2001).
9. Bienkiewicz, E.A. & Lumb, K.J. Random-coil chemical shifts of phosphorylated amino acids. *J. Biomol. NMR* **15**, 203–206 (1999).
10. Ellis, R.J. Macromolecular crowding: an important but neglected aspect of the intracellular environment. *Curr. Opin. Struct. Biol.* **11**, 114–119 (2001).
11. Minton, A.P. The influence of macromolecular crowding and macromolecular confinement on biochemical reactions in physiological media. *J. Biol. Chem.* **276**, 10577–10580 (2001).
12. Murray, A.W. Cell cycle extracts. *Methods Cell Biol.* **36**, 581–605 (1991).
13. Wilhelm, V., Rojas, P., Gatica, M., Allende, C.C. & Allende, J.E. Expression of the subunits of protein kinase CK2 during oogenesis in *Xenopus laevis*. *Eur. J. Biochem.* **232**, 671–676 (1995).
14. Jans, D.A., Ackermann, M.J., Bischoff, J.R., Beach, D.H. & Peters, R. p34cdc2-mediated phosphorylation at T124 inhibits nuclear import of SV-40 T antigen proteins. *J. Cell Biol.* **115**, 1203–1212 (1991).
15. Ferrell, J.E., Jr. *Xenopus* oocyte maturation: new lessons from a good egg. *Bioessays* **21**, 833–842 (1999).
16. Ubersax, J.A. & Ferrell, J.E.,, Jr. Mechanisms of specificity in protein phosphorylation. *Nat. Rev. Mol. Cell Biol.* **8**, 530–541 (2007).
17. Gautier, J., Matsukawa, T., Nurse, P. & Maller, J. Dephosphorylation and activation of *Xenopus* p34cdc2 protein kinase during the cell cycle. *Nature* **339**, 626–629 (1989).
18. Selenko, P., Serber, Z., Gadea, B., Ruderman, J. & Wagner, G. Quantitative NMR analysis of the protein G B1 domain in *Xenopus laevis* egg extracts and intact oocytes. *Proc. Natl. Acad. Sci. USA* **103**, 11904–11909 (2006).
19. Ferrell, J.E., Jr. & Bhatt, R.R. Mechanistic studies of the dual phosphorylation of mitogen-activated protein kinase. *J. Biol. Chem.* **272**, 19008–19016 (1997).
20. Niefind, K., Yde, C.W., Ermakova, I. & Issinger, O.G. Evolved to be active: sulfate ions define substrate recognition sites of CK2α and emphasise its exceptional role within the CMGC family of eukaryotic protein kinases. *J. Mol. Biol.* **370**, 427–438 (2007).
21. Sarno, S., Vaglio, P., Cesaro, L., Marin, O. & Pinna, L.A. A multifunctional network of basic residues confers unique properties to protein kinase CK2. *Mol. Cell. Biochem.* **191**, 13–19 (1999).
22. Cox, S., Radzio-Andzelm, E. & Taylor, S.S. Domain movements in protein kinases. *Curr. Opin. Struct. Biol.* **4**, 893–901 (1994).
23. Bhattacharyya, R.P., Remenyi, A., Yeh, B.J. & Lim, W.A. Domains, motifs, and scaffolds: the role of modular interactions in the evolution and wiring of cell signaling circuits. *Annu. Rev. Biochem.* **75**, 655–680 (2006).
24. Remenyi, A., Good, M.C. & Lim, W.A. Docking interactions in protein kinase and phosphatase networks. *Curr. Opin. Struct. Biol.* **16**, 676–685 (2006).
25. Pawson, T. & Scott, J.D. Signaling through scaffold, anchoring, and adaptor proteins. *Science* **278**, 2075–2080 (1997).
26. Marin, O. *et al.* Tyrosine versus serine/threonine phosphorylation by protein kinase casein kinase-2. A study with peptide substrates derived from immunophilin Fpr3. *J. Biol. Chem.* **274**, 29260–29265 (1999).
27. Marin, O., Meggio, F. & Pinna, L.A. Structural features underlying the unusual mode of calmodulin phosphorylation by protein kinase CK2: a study with synthetic calmodulin fragments. *Biochem. Biophys. Res. Commun.* **256**, 442–446 (1999).
28. Sattler, M., Schleucher, J. & Griesinger, C. Heteronuclear multidimensional NMR experiments for the structure determination of proteins in solution employing pulsed field gradients. *Prog. Nucl. Magn. Reson. Spectrosc.* **34**, 93–158 (1999).
29. Frueh, D.P., Arthanari, H. & Wagner, G. Unambiguous assignment of NMR protein backbone signals with a time-shared triple-resonance experiment. *J. Biomol. NMR* **33**, 187–196 (2005).
30. Sun, Z.Y., Frueh, D.P., Selenko, P., Hoch, J.C. & Wagner, G. Fast assignment of (15) N-HSQC peaks using high-resolution 3D HNcocaNH experiments with non-uniform sampling. *J. Biomol. NMR* **33**, 43–50 (2005).
31. Rovnyak, D. *et al.* Accelerated acquisition of high resolution triple-resonance spectra using non-uniform sampling and maximum entropy reconstruction. *J. Magn. Reson.* **170**, 15–21 (2004).
32. Haas, W. *et al.* Optimization and use of peptide mass measurement accuracy in shotgun proteomics. *Mol. Cell. Proteomics* **5**, 1326–1337 (2006).
33. Yates, J.R. III, Eng, J.K., McCormack, A.L. & Schieltz, D. Method to correlate tandem mass spectra of modified peptides to amino acid sequences in the protein database. *Anal. Chem.* **67**, 1426–1436 (1995).
34. Beausoleil, S.A., Villen, J., Gerber, S.A., Rush, J. & Gygi, S.P. A probability-based approach for high-throughput protein phosphorylation analysis and site localization. *Nat. Biotechnol.* **24**, 1285–1292 (2006).
35. Schwieters, C.D., Kuszewski, J.J., Tjandra, N. & Clore, G.M. The Xplor NIH NMR molecular structure determination package. *J. Magn. Reson.* **160**, 65–73 (2003).

Supplementary Figure 1

In situ observation of protein phosphorylation by high-resolution NMR spectroscopy.

Philipp Selenko, Dominique P. Frueh, Simon J. Elsaesser, Wilhelm Haas, Steven P. Gygi and Gerhard Wagner

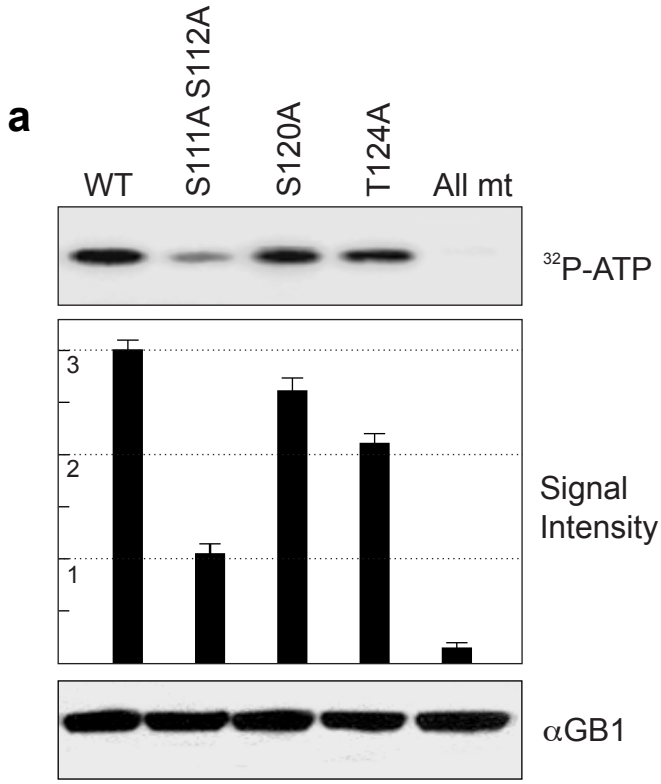

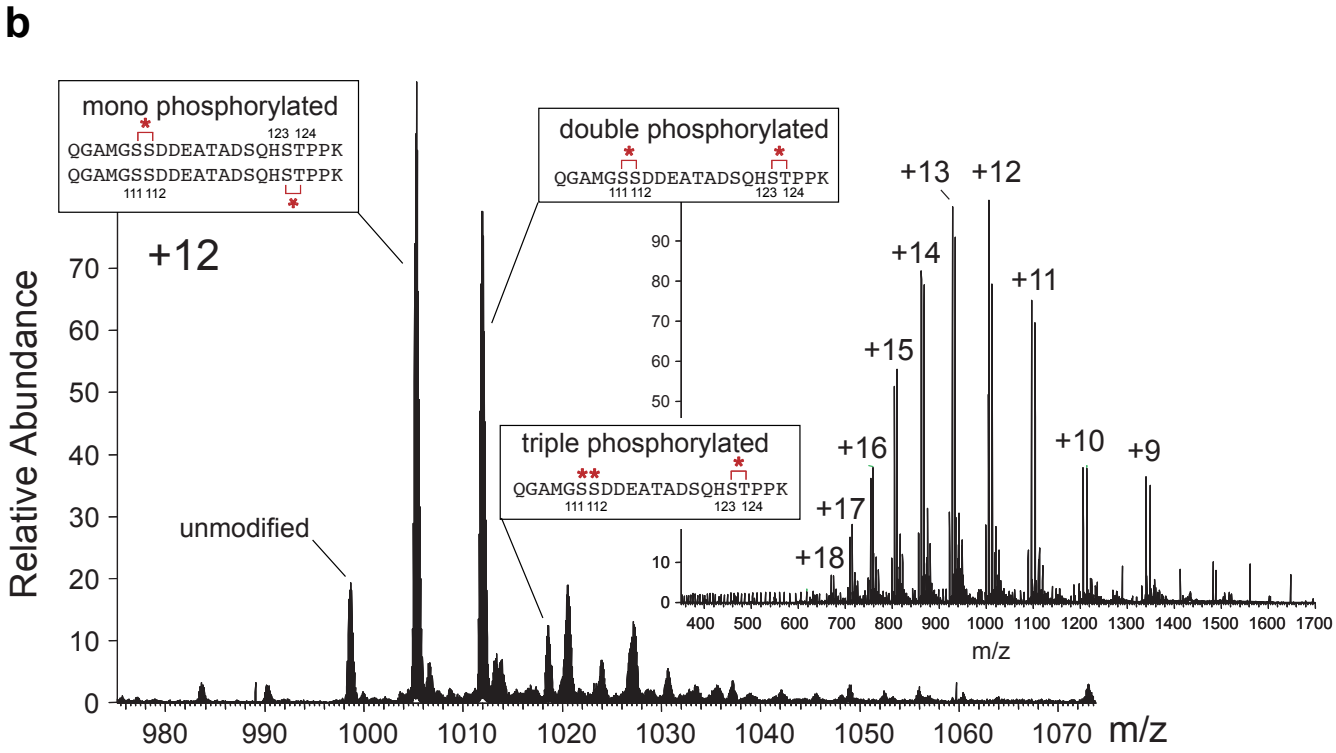

Supplementary Figure 1: Verification of $XT_{111-132}GB1$ phosphorylation by endogenous kinases in *Xenopus* egg extracts. (**a**) $XT_{111-132}GB1$ [γ-^{32}P] ATP incorporation assays in *Xenopus* egg extracts employing wild type (wt) and mutant substrates. The top panel shows the actual [γ-^{32}P] signals of incorporated ATP, obtained after extract incubation for 160min and the respective pull-down experiments. Shown are wt $XT_{111-132}GB1$, the double CK2 site mutant S111A/S112A, S120A and the Cdk1 site mutant T124A. The middle panel displays a quantification of relative [γ-^{32}P] ATP levels from duplicate incorporation experiments. Wt signal intensities were arbitrarily set to three. Western Blot analyses confirmed equal protein quantities of all substrates after the respective pull-down reactions (bottom panel). No [γ-^{32}P] ATP incorporation was observed in control experiments omitting *Xenopus* egg extracts (data not shown). (**b**) Fourier transform ion cyclotron resonance (FT-ICR) mass spectrometry of egg extract-modified $XT_{111-132}GB1$. Phosphorylated $XT_{111-132}GB1$ was purified from extracts after 100min of incubation to yield a mixture of unmodified-, Ser112 and Thr124 phosphorylated-, as well as Ser112, Ser111 and Thr124 phosphorylated, -substrates. The mixed population sample was then subjected to nano-scale micro-capillary reversed (C_4) liquid chromatography on-line coupled to an FT-ICR mass spectrometer (LC-MS). The shown mass spectrum at the right is the average of 109 spectra acquired over the course of four poorly resolved chromatographic peaks (data not shown) and displays multiple positively charged ion species (+9 to +18) of the eluted protein forms. An extended region of a single charge state (+12) of the different protein forms is shown on the left.

Unmodified (u), mono (m), doubly (d), and triply (t) phosphorylated $XT_{111\text{-}132}GB1$ was detected (see annotated peaks). The determined masses for the different forms, the deviation from the theoretical masses, and the semi-quantitatively measured relative amount of the different forms were: (u) 11971.68Da (average mass), 23ppm, 15%; (m) 12051.67Da, 22ppm, 45%; (d) 12131.67Da, 20ppm, 35%; (t) 12211.65Da, 20ppm, 5%. To determine the specific phosphorylation sites, modified $XT_{111\text{-}132}GB1$ was digested with trypsin and the generated peptide mixture analyzed by liquid chromatography tandem mass spectrometry (LC-MS/MS). MS/MS spectra were assigned using the SEQUEST algorithm. Partial sequences of the four identified phosphopeptides are boxed. Asterisks indicate unambiguously determined phosphorylation sites. Mono phosphorylated species were identified as being modified on either Ser111 or Ser112, or on Ser123 or Thr124. The MS/MS data did not allow an exact assignment of these modifications to either of the two residues, but confirmed that residues comprising the CK2 and Cdk1 sites could be independently phosphorylated by endogenous *Xenopus* kinases. The doubly phosphorylated peptide was modified on Ser111 or Ser112 and on Ser123 or Thr124, whereas phosphorylation of the triply modified species was detected on Ser111, Ser112, and on either Ser123 or Thr124. In accordance with the [γ-^{32}P] ATP incorporation assays shown in (a), no phosphorylation of Ser120 was detected in *Xenopus* egg extracts.

Supplementary Figure 2

In situ observation of protein phosphorylation by high-resolution NMR spectroscopy.

Philipp Selenko, Dominique P. Frueh, Simon J. Elsaesser, Wilhelm Haas, Steven P. Gygi and Gerhard Wagner

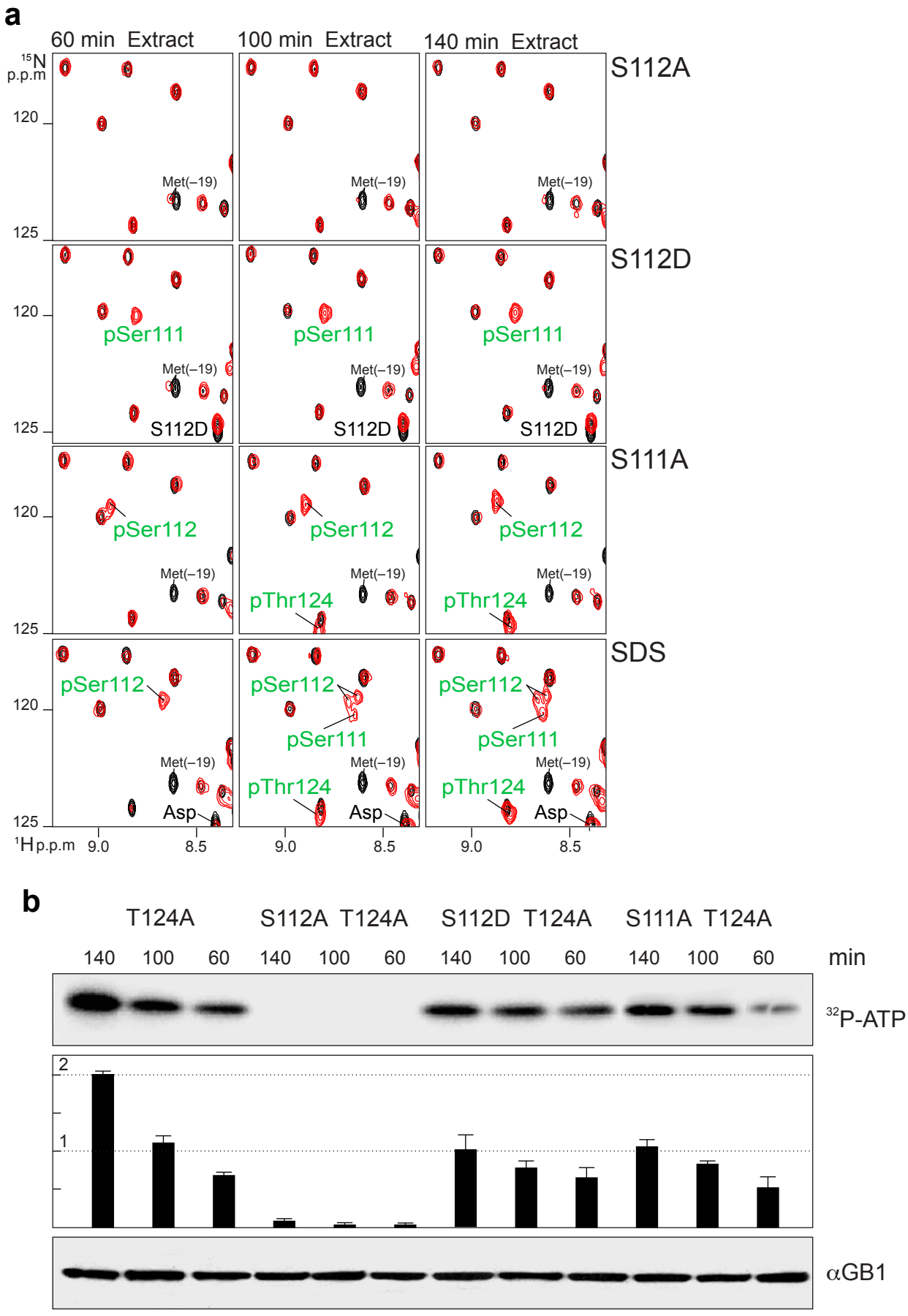

Supplementary Figure 2: Mutational analyses of the stepwise phosphorylation cascade at Ser112 and Ser111 in *Xenopus* egg extracts. (**a**) A serine to alanine substitution of the SV40 residue Ser112 (S112A) effectively suppressed phosphorylation of neighboring Ser111 in egg extracts, even at extended incubation times (140min). Mimicking phosphorylation at Ser112 by a serine to aspartate substitution (S112D) resulted in the immediate modification of Ser111 in extracts. Mutating Ser111 to alanine (S11A) had no effect on the initial phosphorylation reaction of Ser112. Inserting an aspartic acid residue in between Ser111 and Ser112 (SDS) still resulted in the initial phosphorylation of Ser112. (**b**) [γ-^{32}P] ATP incorporation assays in *Xenopus* egg extracts with different T124A mutant substrates (The T124A mutant background was chosen to unambiguously and exclusively resolve phosphorylation events at CK2 site residues). The [γ-^{32}P] ATP signal of T124A after 140min of extract incubation was arbitrarily set to two and all other intensities were determined relative to this value. S112D/T124A and S111A/T124A incorporated half the amount of [γ-^{32}P] ATP than T124A alone, which indicated that in these constructs only one residue became phosphorylated (Ser111 and Ser112, respectively). The S112A/T124A mutant did not exhibit detectable levels of [γ-^{32}P] ATP incorporation at all time points. Western Blot analyses confirmed equal protein quantities for all substrates after the pull-down reactions (bottom panel).

Supplementary Figure 3

In situ observation of protein phosphorylation by high-resolution NMR spectroscopy.

Philipp Selenko, Dominique P. Frueh, Simon J. Elsaesser, Wilhelm Haas, Steven P. Gygi and Gerhard Wagner

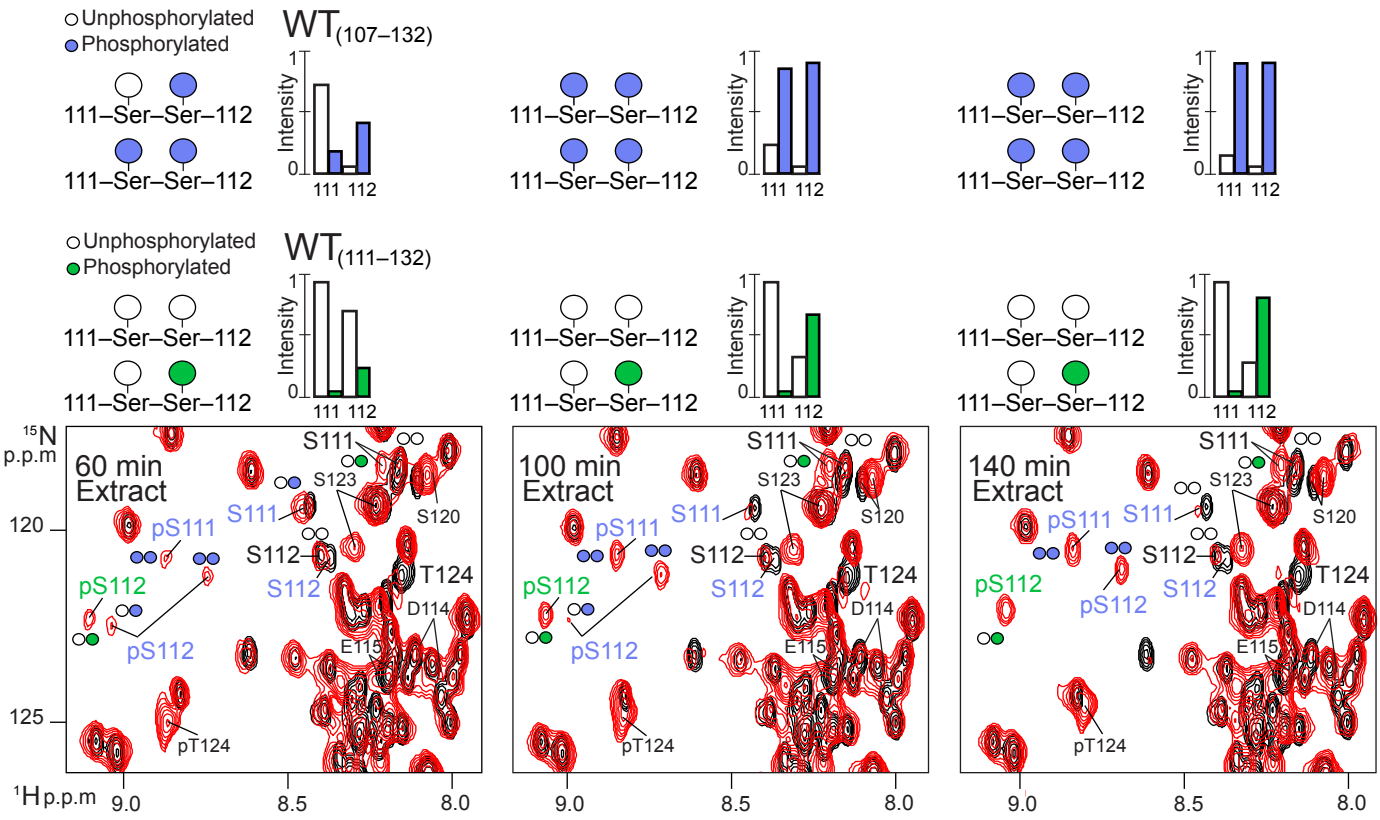

Supplementary Figure 3: Extract NMR analyses of CK2 phosphorylation profiles of a mixed sample of ^{15}N labeled $XT_{111-132}GB1$ (50μM) and $XT_{107-132}GB1$ (50μM). Because NMR peaks of unmodified and modified Ser112 and Ser111 in $XT_{111-132}GB1$ and $XT_{107-132}GB1$ display different resonance frequencies, a mixture of both substrates could simultaneously be analyzed and individual phosphorylation events unambiguously detected. (Note that most GB1 resonances from both substrates overlap due to identical chemical environments in the GB1 moieties. This gives rise to double NMR signal intensities for GB1 resonances since the effective NMR concentration of these residues is determined by the sum of the individual substrate concentrations i.e. 100μM. The same is true for the combined resonance signals of unmodified and phosphorylated Thr124). Phosphorylation of Ser112 and Ser111 of $XT_{107-132}GB1$ is annotated in blue, whereas the modification of Ser112 and Ser111 of $XT_{111-132}GB1$ is shown in black and green. Individual signal intensities were quantified separately and are shown in the top panels of the figure. As can be appreciated from the time course NMR experiment, phosphorylation of Ser112 and Ser111 of $XT_{107-132}GB1$ proceeded with a similar kinetic profile as under 'isolated' conditions in *Xenopus* egg extracts (compare to **Fig. 5c**). In contrast, phosphorylation of Ser112 of $XT_{111-132}GB1$ pursued at a greatly reduced rate. After 140min of extract incubation a residual NMR signal of unmodified $XT_{111-132}GB1$/Ser112 was still detected. Under 'isolated' conditions, and at equivalent incubation times, Ser112 and Ser111 of $XT_{111-132}GB1$ were fully phosphorylated (compare to **Fig. 5b**).